

Increased manganese superoxide dismutase (SOD-2) is part of the mechanism for prostate tumor suppression by Mac25/insulin-like growth factor binding-protein-related protein-1

Stephen R Plymate^{*1,2}, Kathy H Haugk¹, Cynthia C Sprenger³, Peter S Nelson^{2,4}, Marie K Tennant¹, Yuping Zhang⁵, Larry W Oberley⁵, Weixiong Zhong^{6,7}, Rolf Drivdahl¹ and Terry D Oberley^{6,7}

¹Veterans Affairs Puget Sound Health Care System, University of Washington School of Medicine, Seattle, WA 98105, USA;

²Department of Medicine, University of Washington School of Medicine, Seattle, WA 98105, USA; ³Department of Molecular and Cell Biology Program, University of Washington School of Medicine, Seattle, WA 98105, USA; ⁴Fred Hutchinson Cancer Research Center, Seattle, WA 98107, USA; ⁵Department of Radiology, University of IA, Iowa City, IA 52242, USA; ⁶Department of Pathology and Laboratory Medicine, University of WI, Madison, WI 53705, USA; ⁷Pathology Service, William S Middleton Memorial Veterans Hospital, Madison, WI 53705, USA

Increased expression of mac25/insulin-like growth factor binding-protein related protein-1 (IGFBP-rP1) in human breast and prostate epithelial cell lines results in the suppression of tumor growth. CDNA expression array analysis revealed increased manganese superoxide dismutase (SOD-2) expression in the mac25/IGFBP-rP1-transfected M12 human prostate cancer cell line compared to M12 control cells. SOD-2 has been postulated to be a tumor suppressor. SOD-2 was also increased in LNCaP cells stably transfected with mac25/IGFBP-rP1, but not in mac25/IGFBP-rP1-transfected PC-3 cells. Mac25 LNCaP cells had a marked decrease in tumor growth in nude mice compared to controls, but there was no difference in tumor growth in mac25 PC-3 cells compared to control. Phosphorylated Erk and Akt were increased in the M12 and LNCaP transfected mac25/IGFBP-rP1 cells but not PC-3 mac25. Inhibition of PI-3 kinase results in a marked decrease in viability of the M12-mac25 cells compared to M12 controls. Cells treated with H₂O₂ result in an increase in phospho-ERK. Transfection of SOD-2 in M12 cells markedly decreased tumor growth, apoptosis, G1 delay in the cell cycle, and expression of senescence associated β -galactosidase. These results suggest that one of the downstream mediators of the senescence-associated tumor suppression effect of mac25/IGFBP-rP1 is SOD-2.

Oncogene (2003) 22, 1024–1034. doi:10.1038/sj.onc.1206210

Keywords: SOD-2; Mac25; prostate; cancer; IGFBP-rP1

Introduction

Mac 25, also termed insulin-like growth factor binding-protein-related protein-1 (IGFBP-rP1), is a senescence-associated gene that demonstrates decreased expression in prostate cancer (Hwa *et al.*, 1998a). Re-expression of mac25/IGFBP-rP1 in malignant human prostate epithelial cells with the potential to undergo senescence results in a marked decrease in tumor growth compared to control cells in nude mice tumor injection studies (Sprenger *et al.*, 1999). The mechanism by which mac25/IGFBP-rP1 suppresses tumor growth has recently been shown to involve the inhibition of cell-cycle progression at G1 and enhanced apoptosis. The increased apoptosis is associated with the unscheduled expression of cyclin A (Sprenger *et al.*, 2002). In addition to decreased tumor growth, re-expression of mac25/IGFBP-rP1 results in the expression of senescence-associated β -galactosidase that is consistent with the expression of mac25/IGFBP-rP1 in senescent prostate epithelial cells (Lopez-Bermejo *et al.*, 2000). Thus, mac25/IGFBP-rP1's function as a tumor suppressor gene occurs, in part, through induction of cell senescence.

Recent data demonstrate that mac25/IGFBP-rP1 is targeted to the nucleus and is a potential transcription factor (Wilson *et al.*, 2001). This suggests the possibility that mac25/IGFBP-rP1 may have its phenotypic activity induced through the activity of downstream genes. In this study, we used cDNA expression arrays to search for genes induced by mac25/IGFBP-rP1 that are involved in the senescence process. Among the genes that were induced, superoxide dismutase-2 (SOD-2, manganese superoxide dismutase) was of interest because deHaan *et al.* (1996) have shown that SOD-1 (Cu/ZnSOD) has the potential to induce apoptosis through the generation of hydrogen peroxide (H₂O₂). Since administration of H₂O₂ directly to cells will induce senescence, as defined by an increase in senescence-

*Correspondence: SR Plymate, Harborview Medical Center, Box 359755, 325 9th Avenue, Seattle, WA 98104, USA;
E-mail: splymate@u.washington.edu
Received 27 August 2002; revised 31 October 2002; accepted 4 November 2002

associated β -galactosidase expression and a change in cell morphology, SOD-2 should also potentially be able to induce senescence via H_2O_2 production (Chen *et al.*, 1998). SOD-2 expression is decreased in the progression from benign to malignant prostate epithelium, and when re-expressed in human prostate cancer cell lines causes tumor regression (Baker *et al.*, 1997; Li *et al.*, 1998b; Bostwick *et al.*, 2000). At least one mechanism by which SOD-2 decreases tumor growth is by causing a delay at G0/G1 in the cell cycle (Li *et al.*, 1998b; Oberley, 2001). In addition to the action of SOD-2 in prostate cancer, the antioxidant properties of SOD-2 make it an enzyme of general interest in cancer prevention and tumor suppression (Oberley and Oberley, 1997; Oberley, 2001; Zhong and Oberley, 2001).

Results

Cell lines

In addition to the M12 cell lines expressing mac25/IGFBP-rP1 that have been reported previously, in this study the transfection of mac25/IGFBP-rP1 into LNCaP and PC-3 cells resulted in clones that expressed mac25/IGFBP-rP1 levels between 5–10-fold above those of the wild-type parental cells (Figure 1) (Sprenger *et al.*, 1999).

Alterations in gene expression mediated by mac25/IGFBP-rP1

cDNA microarray analysis of M12 cells was performed to identify transcriptional alterations resulting from the expression of mac25/IGFBP-rP1. Of approximately 6000 genes assayed, 12 exhibited reproducible transcriptional alterations of two-fold or greater (Table 1). Of these, the expression of SOD-2 increased 3.33-fold in cells transfected with mac25/IGFBP-rP1 relative to controls. SOD-2 is involved in the generation of H_2O_2 from superoxide in mitochondria. SOD-2 also causes cells to develop a senescent phenotype and causes growth inhibition of tumor cells *in vivo* and *in vitro*. Therefore, SOD-2 was selected as a potential mediator of some of the functions of mac25/IGFBP-rP1 in prostate epithelial cells.

The differences in expression of SOD-2 between the M12 control cells and the mac25/IGFBP-rP1 M12 cells were confirmed by Northern and Western analyses, (Figure 1). Enzymatic SOD activity was significantly increased in M12-mac25/IGFBP-rP1 and M12-SOD-2 sense compared to M12 control cells (Figure 2), whereas SOD-2 mRNA and immunoreactive protein and total SOD enzymatic activity was decreased in M12 antisense (AS) cells compared to M12 control cells (Figure 1b). Specific SOD-2 assays confirmed that the differences in SOD activity between cell constructs were because of SOD-2 (data not shown).

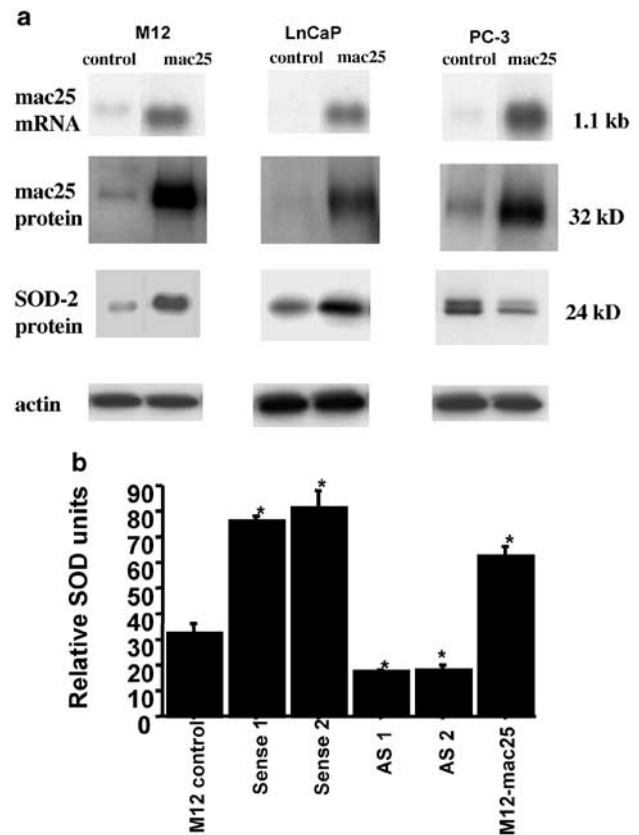


Figure 1 Northern and Western blots and total SOD bioassay demonstrating an increase in SOD-2 expression associated with transfection of mac25/IGFBP-rP1 into M12 and LNCaP, but not PC-3, cells. (a) Northern and Western analyses of cytoplasmic RNA and cell lysate, respectively, from representative clones of M12-, LNCaP-, and PC-3-control cells compared to the same cell lines transfected with mac25/IGFBP-rP1 (M12-mac25, LNCaP-mac25, and PC-3-mac25). Northern analyses were probed with mac25/IGFBP-rP1 cDNA and Western analyses with an anti-mac25/IGFBP-rP1 and anti SOD-2. Note the marked increase in mac 25 and SOD-2 expression in each of the transfected cell lines except for PC-3 mac25/IGFBP-rP1 that showed a marked decrease in SOD-2. Cells were grown in complete RPMI medium described in Materials and methods without FCS. Actin was used as a loading control for Western analyses and Northern analysis RNA was evenly loaded as determined by ethidium bromide stained 28S ribosomal RNA (data not shown). (b) Mean levels SOD enzymatic activity in M12-control, M12-mac25, M12-SOD-2 sense, and M12-SOD-2 antisense cells. * = $P \leq 0.01$ compared to M12 control cells

Mac25/IGFBP-rP1 expression in PC-3 and LNCaP cells

In order to determine if SOD-2 was induced in response to increased mac25/IGFBP-rP1 expression in other human prostate epithelial cancer cell lines, we constructed clones of LNCaP and PC-3 cells expressing mac 25/IGFBP-rP1 (Figure 1a). Similar to our previous observation with M12 cells, the LNCaP cells had an increase in senescence as determined by the detection of SA- β galactosidase. In contrast, there was no difference in SA- β galactosidase expression between parental PC-3 cells and those expressing mac25/IGFBP-rP1. SOD-2 expression was increased in the mac25/IGFBP-rP1-

Table 1 Genes regulated by mac25/IGFBP-rP1 expression in M12 cells. Gene name and NCBI-GeneBank ID

Gene	Δ Fold	Accession	Description
VIM	9.2	NM_003380	Vimentin
LOC95665	5.3	XM_051780	PGP 9.5 similar to ubiquitin carboxyl-terminal hydrolase L1
APACD	4.3	NM_005783	ATP binding protein
IGFBP-7	3.5	NM_001553	Mac25/IGFBP-7/IGFBP-rP1
IL8	3.4	NM_000584	Interleukin-8
SOD-2	3.3	NM_000636	Mn superoxide dismutase
IDH2	2.8	NM_002168	Mitochondrial isocitrate dehydrogenase 2
SOX9	2.7	NM_000346	Sex determining region Y-box 9
VACX	2.1	NM_015994	Vacuolar ATPase
CD9	-2.4	NM_001769	CD-9 antigen (p24)
AGR2	-2.8	NM_006408	Anterior gradient 2 homolog
KRT8	-4.0	NM_002273	Cytokeratin 8

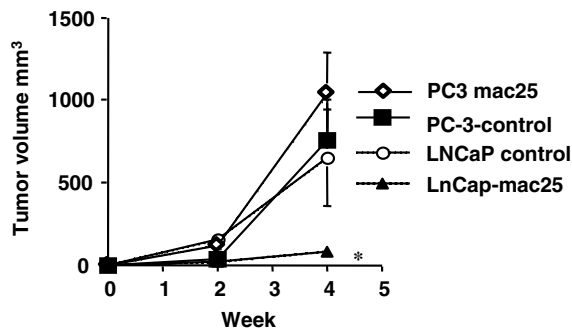


Figure 2 Mac25/IGFBP-rP1 expression suppresses growth of LNCaP cells in nude mice, but has no effect on PC-3 cells. Tumor volume of PC-3, control and PC-3-mac25 or LNCaP control and LNCaP mac25 cells injected s.c. in the flank of nude mice. There was no difference in tumor volume between PC-3 control, PC-3 mac25, or LNCaP control cells. LNCaP mac25 cells had significantly decreased tumor volume compared to LNCaP controls. * = $P \leq 0.01$ compared to control

expressing LNCaP clones, but SOD-2 was decreased in the PC-3 cells (Figure 1). Finally, there was no difference in tumor volume in the mac25/IGFBP-rP1-expressing PC-3 cells, compared to parental cells, whereas the mac25/IGFBP-rP1-transfected LNCaP cells demonstrated a marked decrease in tumor volume compared to LNCaP control cells, similar to the effects previously reported in M12 cells, Figure 2 (Sprenger *et al.*, 1999, 2002).

SOD-2 expression in M12 cells

In order to determine if the expression of SOD-2 could account for some of the phenotypic findings noted from expression of mac25/IGFBP-rP1 in M12 and LNCaP, we selected clones of M12 cells transfected with pcDNA3 containing SOD-2 ligated in either a sense or antisense direction. As noted in Figure 3, SOD-2 was markedly overexpressed in the sense clones, whereas SOD-2 expression was decreased in the antisense clones. SOD enzymatic activity was also significantly different between clones made with either sense or antisense constructs as noted in Figure 1b. This assay measures total SOD enzymatic activity and it is possible that other SOD forms also changed with transfection of SOD-2;

however, no changes in CuZnSOD expression was noted on Western analysis (data not shown) and catalase expression was not altered Figure 3. SOD enzymatic activity was significantly increased in M12-mac25 expressing cells and M12-SOD 2 sense cells compared to M12 control cells; whereas enzymatic activity was significantly decreased in the SOD-2 antisense cells compared to controls (Figure 1b). In addition to total SOD activity, specific SOD-1 and SOD-2 activities were measured in the M12 cells expressing mac25/IGFBP-rP1 and M12 control cells. SOD-1 levels were 26.7 and 20.6 U and SOD-2 levels were 40 and 6.7 in M12 cells expressing mac25/IGFBP-rP1 and M12 control cells, respectively.

Growth rate and apoptosis in M12 SOD cells

Growth rates of two M12 SOD-2 sense clones and two M12 SOD-2 antisense clones were determined by cell counts from triplicate wells at 24 h intervals from 24 to 96 h after plating. As shown in Figure 4a, the growth rates for the SOD-2 cells were significantly slower ($P \leq 0.01$) than those obtained from the M12 control and SOD-2 antisense cell lines. Since our previous studies had indicated that the expression of mac 25/IGFBP-rP1 resulted in both inhibition of the cell cycle and an increase in apoptosis, we also examined apoptosis in parallel cultures from the same clones used for proliferation studies. As shown in Figures 4b and c, there was a significant difference in apoptosis between the cell lines based on cleavage of caspases 3 and 7. Although cells can potentially recover following caspase 3 cleavage, this cleavage occurs during a later stage in the apoptotic pathway and since cell viability and cell number are decreased, it is very likely that the decrease in viable cell numbers is due, at least in part, to apoptosis. The SOD-2 sense cells also demonstrated an increase in cleaved PARP, further indicating activation of an apoptotic pathway (data not shown). Apoptosis assays were performed at 21% O_2 concentration.

Tumor Growth in Nude Mice of Cells Overexpressing SOD-2

There was a marked decrease in tumor volume in the M12 SOD-2 sense clones compared to M12

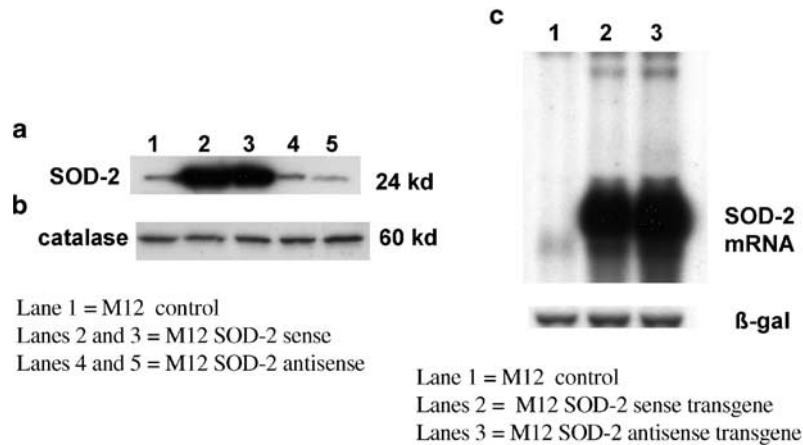


Figure 3 Northern analysis and Western immunoblot of cell lysates from M12 control and two clones of M12-SOD-2 sense and M12-SOD-2 antisense stable cell transfectants demonstrating increased expression of SOD-2 following transfection of a SOD-2 expression vector. Blots were probed with antibody to SOD-2 (a) or catalase (b). The blot is overexposed for the sense constructs in order to allow M12 control and M12-antisense SOD-2 to become visible. Protein loading was controlled as previously described. Note the increase in SOD-2 protein levels in the sense cells compared to controls and the decreased SOD-2 levels in the antisense transfectants. Also note that catalase levels remained stable. (c) Northern analysis demonstrating the SOD-2 sense and antisense transgene expression in M12 cells. Appropriate orientation of the cDNA insert was confirmed with restriction analysis

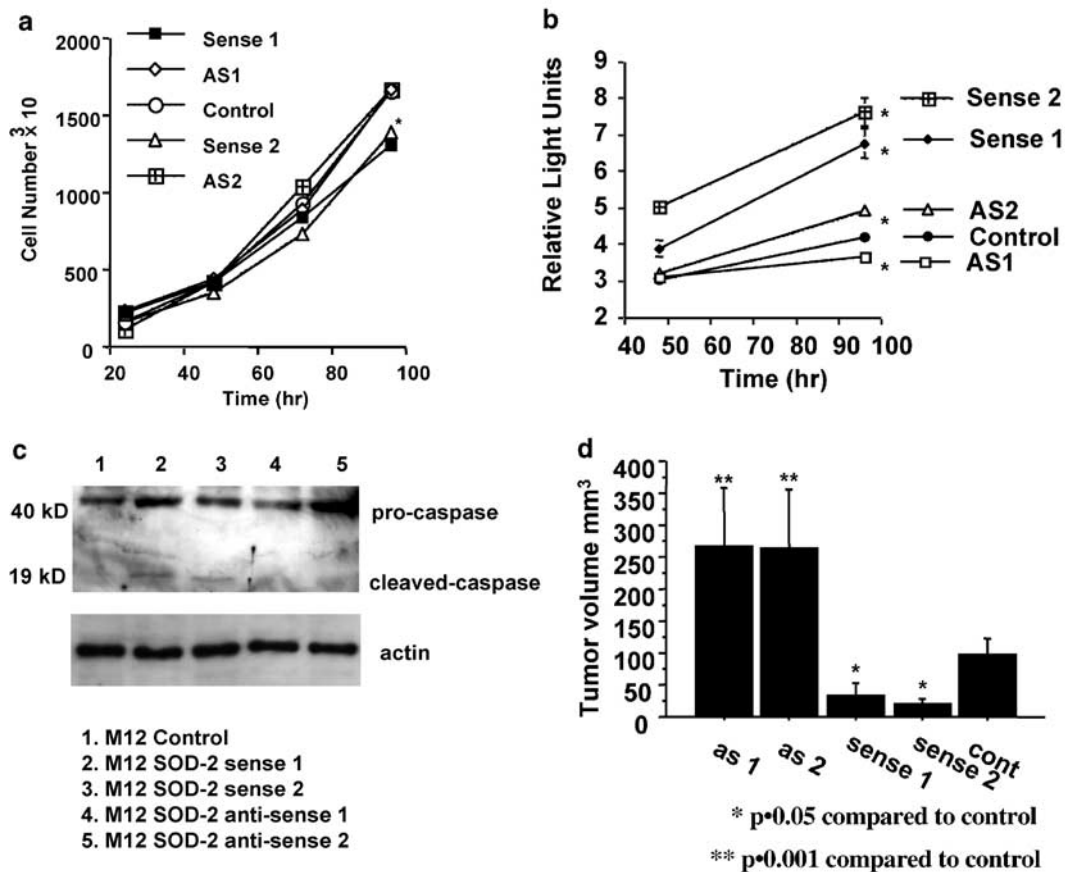


Figure 4 Demonstration of the effects of SOD-2 on cell and tumor growth and apoptosis of M12 cells. Growth rate (a) and apoptosis (b) *in vitro* of SOD-2 sense and antisense cell lines. There was a significant decrease in growth in sense compared to antisense and control cells, whereas apoptosis was increased in sense cells compared to antisense and control cells. Control cells had a greater level of apoptosis than antisense cells. * = $P \leq 0.01$ compared to M12-SOD-2 sense cells. (c) Western immunoblot of cell lysates grown in serum-free medium for 96 h. Lysates were run on a 10% PAGE and probed with an antibody to caspase-3 (Promega Co., Madison, WI, USA). Note the presence of cleaved caspase in the two SOD-2 sense cell lines, but absence of detectable caspase cleavage in M12 control and SOD-2 antisense (AS) cells. Actin was used as a loading control. (d) Tumor volume 6 weeks following injection of 1×10^6 cells s.c. in nude mice of M12 control, M12-SOD-2 sense, and M12-SOD-2 antisense. * = $P \leq 0.05$ ** ≤ 0.01 compared to control

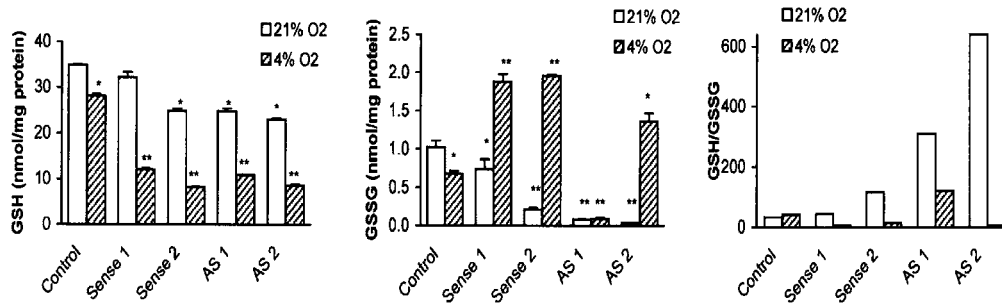


Figure 5 Glutathione (GSH) and reduced glutathione (GSSG) levels in M12 cells vary depending on SOD-2 expression. Alterations of intracellular levels of GSH (a), GSSG (b), and the ratio of GSH : GSSG (c) by overexpression or suppression of MnSOD in M12 cells. Data represent mean \pm s.d., $n=3$. * $P<0.05$ and ** $P<0.01$ compared with control in 21 or 4% O₂

control and antisense clones. In the M12 SOD-2 antisense cell lines, tumor volume was significantly greater than the M12 control and M12 SOD-2 sense cell lines (Figure 4d).

Flow cytometry using propidium iodide

The results of the flow cytometry data demonstrated that 40 ± 4 (s.e.m) % of the M12 control DNA resided in G0/G1, while $55 \pm 3\%$ of the M12 SOD-2 cells from sense clones 1 and 2 resided in G0/G1. These data indicate a delay at G0/G1 of the cell cycle. Further, $7.1 \pm 1\%$ of the DNA from the M12 SOD-2 sense cells was in the sub-G0 area consistent with apoptotic or necrotic cells compared to $3.0 \pm 0.5\%$ of the M12 control cells. These data are consistent with the increased apoptosis in M12 SOD-2 sense cells determined by caspase 3/7 cleavage.

Results of GSH/GSSG assays

To assess intracellular redox state, cellular GSH and GSSG were measured by spectrophotometry in both 21 and 4% concentrations of O₂. In this study, 4% O₂ was included because it is the physiological concentration *in vivo* and represents the concentration in the nude mice study. As shown in Figure 5, levels of GSH in all of the MnSOD transfectants, except for the M12 SOD-2 Sense 1, were slightly decreased when cells were grown in 21% O₂. There was a slight decrease in GSH in the control cells grown in 4% O₂ compared with that in 21% O₂. However, levels of GSH were dramatically decreased in all of the transfectants when grown in 4% O₂. Levels of GSSG were decreased in all of the transfectants grown in 21% O₂. In contrast, levels of GSSG were increased in all of the transfectants, except for the AS 2, grown in 4% O₂; the changes were more dramatic in the sense transfectants. The ratio of GSH to GSSG (GSH:GSSG) was slightly increased in the sense transfectants and dramatically increased in the antisense transfectants in 21% O₂. In contrast, GSH:GSSG in 4% O₂ was dramatically decreased in all of the transfectants, except for AS 1 which showed an increase in GSH:GSSG in 4% O₂.

Effect of mac25/IGFBP-rP1, SOD-2, and H₂O₂ on signal transduction

SOD-2 through the generation of H₂O₂ has been demonstrated to alter cell signaling through the phosphorylation of MAP kinase, and the increase in MAP kinase activation has been suggested to play a role in tumor growth (Wartenberg *et al.*, 1999). Therefore, we examined MAP kinase activation to determine if this pathway could, in part, be a mechanism for the activity seen with expression of mac25. M12 mac25/IGFBP-rP1- and SOD-2-expressing cells demonstrated an increase in basal levels of phosphorylated MAP kinase compared to M12 control cells (Figure 6a). Since H₂O₂ has been demonstrated to function as an intracellular signaling molecule, we also examined M12 control cells following addition of H₂O₂ and saw a marked increase in phosphorylation of MAP kinase (Figure 6b). No further increase in MAP kinase phosphorylation was noted in M12 SOD-2 or mac25/IGFBP-rP1 cells with the addition of H₂O₂. Inhibition of MAP kinase with PD 098059, an inhibitor of extracellular receptor kinase 1 and 2, resulted in a small but significant decrease in cell proliferation as determined by the MTT assay (Figure 7). PKB/Akt phosphorylation was also increased in the M12 mac25/IGFBP-rP1 cells and inhibition of PI-3 kinase by LY294002 resulted in a dramatic decline in cell viability when compared to control cells. A similar increase in Akt activity was observed following H₂O₂ administration (data not shown).

SOD-2 expression in M12 cells induces a senescent phenotype

When SOD-2 was expressed in M12 cells they increased SA- β galactosidase staining consistent with a more senescent phenotype (Table 2). We have previously demonstrated that mac25/IGFBP-rP1 expression in M12 cells is associated with an increase in a senescent phenotype (Sprenger *et al.*, 2002).

SOD-2 promoter stimulation in mac25/IGFBP-rP1-expressing cells

In order to determine if the increase seen in SOD-2 occurred through an increase in SOD-2 transcription,

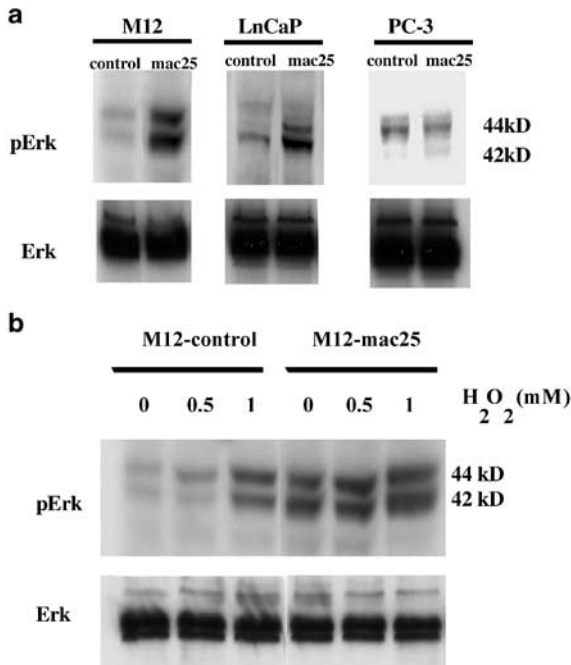


Figure 6 Mac25/IGFBP-rP1 expression in M12 and LnCaP cells and administration of H₂O₂ increase phosphorylation of MAP kinase. (a) Basal levels of total and phosphorylated MAP kinase in representative clones of M12-, LNCaP-, and PC-3-control cells compared to the same cell lines transfected with mac25/IGFBP-rP1 (M12-mac25, LNCaP-mac25, and PC-3-mac25). Note the increase in phosphorylated MAP kinase in M12- and LNCaP-mac25 cells compared to control cell lines. Each experiment was done in triplicate. (b) Western immunoblot of total and phosphorylated MAP kinase following treatment of cells with 1 μM H₂O₂ for 30 min. Note the increase in phosphorylated MAP kinase in M12-control cells following H₂O₂ and no increase in M12-mac25 cells after H₂O₂

Table 2 Per cent of cells expressing β-galactosidase in M12-control and M12-SOD-2 cell lines

Cell line	M12-control	M12-SOD Sense 1	M12-SOD Sense 2
% SA-β gal	4±2	26±5*	32±4*

* = P ≤ 0.001 compared to M12 control.

we transiently transfected a SOD-2 promoter construct in a PGL3-luc reporter plasmid into either M12 control or M12 mac25/IGFBP-rP1-expressing cells. As noted in Figure 8, there was a significant increase in promoter activity in the M12 mac25/IGFBP-rP1-expressing cells when compared to M12 control cells.

Discussion

Recent publications have suggested that mac25/IGFBP-rP1 is transported to the cell nucleus and has a nuclear localization sequence, it may either be a transcription factor or cofactor (Wilson *et al.*, 2001). In this study, we used a cDNA microarray representing 6000 genes

expressed in the prostate to determine if the mac25/IGFBP-rP1 induced expression of genes that are capable of inducing the senescent phenotype. Of the eight genes that were upregulated by mac25/IGFBP-rP1, SOD-2 appeared the most likely candidate. SOD-2 is located in mitochondria and belongs to a family of superoxide dismutase enzymes that converts superoxide radicals to H₂O₂, which is subsequently converted by catalase or glutathione peroxidase to H₂O and O₂ (McCord, 2000; Oberley, 2001). In addition to functioning as an antioxidant, SOD-2-also participates in cell signaling pathways by H₂O₂ production (Rhee *et al.*, 2000). It should be noted that SOD-2-transfected cells can adapt to the transfection and not increase their production of H₂O₂ by decreasing SOD-1 or increasing catalase or GPX(Li *et al.*, 1998b). This adaptation did not appear to occur in our cells since Western analysis of SOD-1 and catalase was unchanged. H₂O₂ has been shown to induce features of the senescent cell phenotype including G1 cell cycle arrest, decreased phosphorylation of retinoblastoma protein (pRb), expression of SA β-galactosidase, and cell enlargement. In a previous publication, we have shown that all of these features except cell enlargement occur in M12 cells expressing mac25/IGFBP-rP1 (Sprenger *et al.*, 2002). In the present study, we sought out which of these features could be explained by mac25/IGFBP-rP1-induced expression of SOD-2, and further, if SOD-2 expression could account for tumor suppression. In the M12 cells in which SOD-2 was expressed, we found an increase in SA-β galactosidase staining, increased MAP kinase and Akt activity with increased dependence on Akt for survival, an increase in p16^{ink} expression, decreased growth rate, and an increase in apoptosis. The increase in SA-β galactosidase was not seen in the antisense SOD-2 cells, further indicating the induction of senescence by SOD-2. Tumor growth in nude mice was markedly suppressed by SOD-2 expression but not to the degree seen with mac25/IGFBP-rP1. This suggests that other functions regulated or influenced by mac25/IGFBP-rP1 also contributed to the inhibition of tumor growth. However, it is important to note that the antisense SOD-2 construct, which inhibited SOD-2 expression, caused a marked increase in the rate of tumor growth. The suppression of growth by SOD-2 expression and stimulation of growth when SOD-2 expression is decreased suggest that SOD-2 is an important regulator of prostate tumor growth. In the PC-3 cells, although SOD-2 is expressed, there were no changes in the level of expression when mac25/IGFBP-rP1 was expressed and no change in tumor growth was noted.

Immunohistochemistry has demonstrated that SOD-2 is decreased in prostate intraepithelial neoplasia and prostate cancer in men. A recent study describing a SOD-2 polymorphism at Val 16 suggested a twofold increased risk for prostate cancer in men with this polymorphism (Sachdeva *et al.*, 2001). Overexpression of SOD-2 in the human prostate cancer cell line DU-145 has also been shown to produce effects similar to those we have described in the M12 cells with slower cell growth because of a delay in G1 of the cell cycle,

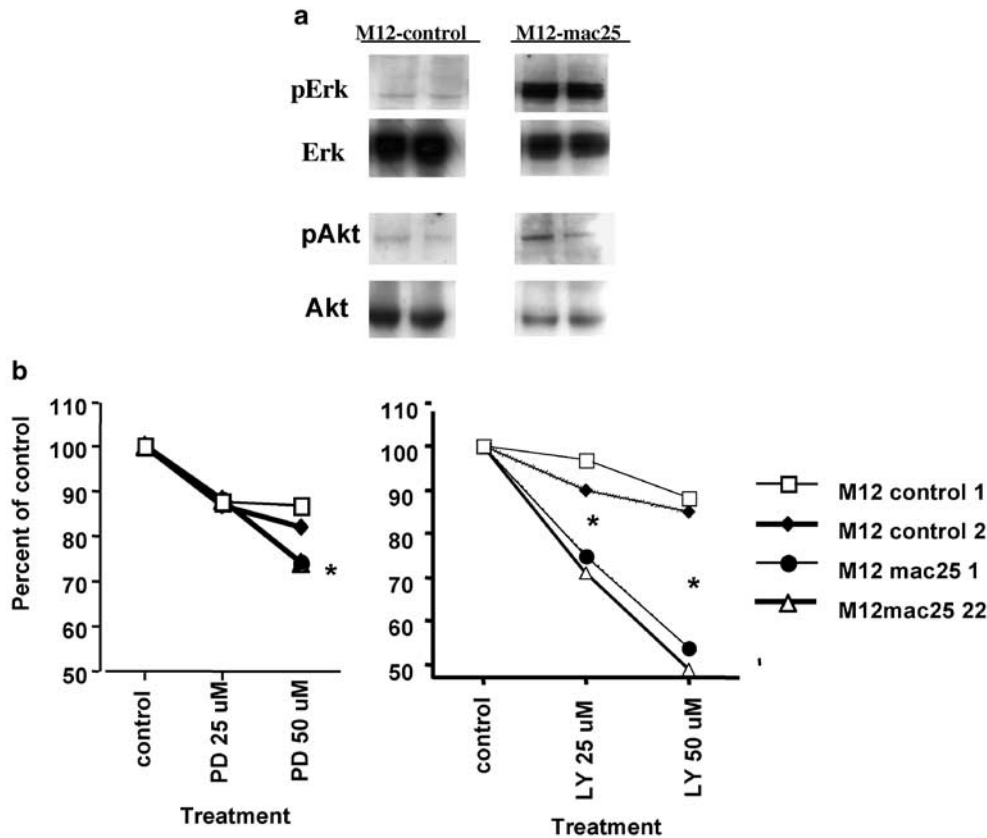


Figure 7 Demonstration of growth inhibition in M12 control and M12-mac25 cells following inhibition of MAP kinase or PI-3 kinase phosphorylation. (a) Western immunoblot of M12-control and a clone of M12-mac25 cells demonstrating total and phosphorylated MAP kinase and PKB/Akt following inhibition of MAP kinase with PD098059 for 24 h or PI3 kinase with LY294002 for 4 h. (b) Cell viability measured following treatment with either PD098059 or LY294002. * = $P \leq 0.01$ compared to control

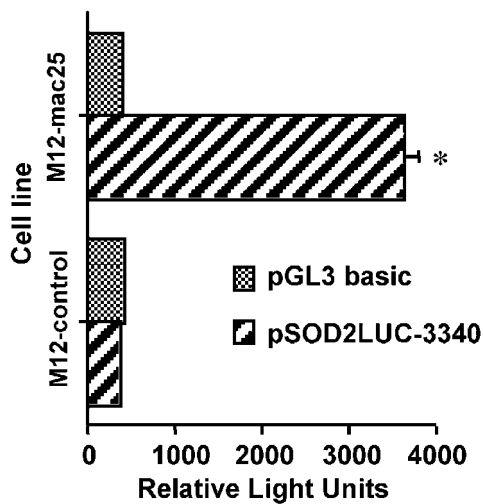


Figure 8 The SOD-2 promoter is activated by mac25/IGFBP-rP1 expression. SOD-2 promoter activity following transient transfection of the SOD-2 promoter construct into either M12-control or M12-mac25 cells. Note the marked increase in promoter activity in M12-mac25 cells compared to control cells. * = $P \leq 0.01$ compared to control

decreased cell viability, and decreased tumor volume in nude mice (Li *et al.*, 1998b). The additional importance of SOD-2 expression on suppression of prostate cancer

growth was recently shown by its induction following selenium administration *in vitro* to LNCaP cells (Zhong and Oberley, 2001). In that study, the increase in SOD-2 following selenium administration was associated with a decrease in apoptosis and a delay at the G2/M cell-cycle checkpoint.

The increase in basal activation of MAP kinase by cells responding to mac25/IGFBP-rP1, SOD-2, or H_2O_2 suggests a pathway by which the generation of H_2O_2 could decrease cell growth. Although acute stimulation of MAP kinase is associated with cell proliferation, chronic elevation of phosphorylated MAP kinase has been associated with decreased cell growth, differentiation, and apoptosis (Birkenkamp *et al.*, 1999; Bost *et al.*, 2002). The mechanisms for these effects are not entirely clear, but have been suggested to involve inhibition of cyclin D and stimulation of p38 MAP kinase. In our studies, the marked increase in phosphorylated MAP kinase was associated with a slight decrease in proliferation when inhibited with PD 095049, but the decrease in cell viability was not nearly as great as that seen with inhibition of PI3 kinase. This suggests that the dependence on PI3 kinase is a response to induction of other cell death pathways by SOD-2 expression. The mechanisms by which SOD-2 can lead to increased cell death have recently been reviewed (Kim *et al.*, 2001;

Oberley, 2001; Sprenger *et al.*, 2002). Our previous data suggest that the apoptosis may be associated with the unscheduled expression of cyclin A (Sprenger *et al.*, 2002). Although studies from many laboratories have demonstrated that SOD-2 inhibits tumor growth through interruption of the cell cycle, the effects on apoptosis have not been as straightforward since some studies have shown protection from apoptosis, while others have demonstrated increased apoptotic cell death (Kim *et al.*, 2001). One potential mechanism for induction of apoptosis in this study could be through the reduced GSH/GSSG ratio in the SOD-2 sense cells. As GSH is consumed and GSSG is produced in excess of GSH, there is a relative change in the redox state of the cell to one of greater oxidation. As the cells are exposed to increased oxidative stress, viability is lost and cell death may occur (Zhong and Oberley, 2001). This change in the redox environment of the mitochondria inhibits pyruvate carboxylase and enhances the toxicity of *NO (Kim *et al.*, 2001). Another mechanism for SOD-2-induced apoptosis is through its ability to activate p53 by the production of H₂O₂ (Huang *et al.*, 2000; Kinscherf *et al.*, 1998). We have demonstrated that expression of mac25/IGFBP-rP1 is associated with activation of p53; therefore, this mechanism of induction of apoptosis by SOD-2 through p53 is relevant to the current model (Sprenger *et al.*, 2002). Additionally, proapoptotic activity may result by signaling via the ras pathway with activation of raf1 as suggested by the increase in MAP kinase phosphorylation. (Widmann *et al.*, 1998).

In summary, this study used transcript profiling methods to identify genes regulated by the expression of mac25/IGFBP-rP1 that are responsible for tumor suppression. It further demonstrates the significance of SOD-2 as a potential regulatory protein in prostate cancer development.

Materials and methods

Materials

Tissue culture media, RPMI-1640, gentamicin, fungizone, geneticin (G418), and deoxyribonuclease were obtained from Life Technologies (Gibco-BRL) (Grand Island, NY, USA). Epidermal growth factor (EGF), dexamethasone, and the additive ITS (insulin, transferrin, selenium) were purchased from Sigma Chemical Co. (St Louis, MO, USA). Fetal bovine serum (FBS) was obtained from Hyclone (Logan, UT, USA). Tfx™-50 Reagent was obtained from Promega (Madison, WI, USA). The BCA protein assay kit was from Pierce Biological (Rockford, IL, USA). The IGFBP-rP1 cDNAs were obtained as previously described from a cDNA library made from the human breast carcinoma cell line, Hs578T (Oh *et al.*, 1996). Mac25/IGFBP-rP1 polyclonal anti-rabbit antibody was provided as a generous gift by Drs V Hwa and R Rosenfeld at Oregon Health Sciences University, Portland OR. Characterization of this antibody in our laboratory has been previously described (Hwa *et al.*, 1998b). SOD-2 antibody was purchased from Upstate Biological (Lake Placid, NY, USA) and actin antibody was from Santa Cruz Biotechnology (Santa Cruz, CA, USA). Horseradish peroxidase-linked donkey anti-rabbit

IgG and enhanced chemiluminescence (ECL) detection reagents were purchased from Amersham (Arlington Heights, IL, USA). Each experiment was performed at least three separate times. SOD-2 human cDNA was I.M.A.G.E. Consortium clone 124182 was from ATCC (Manassas, VA, USA). The cDNA was cut with *Eco*R1(5') and *Hind*III (3') restriction enzymes and subsequently ligated into pcDNA 3.1+ and -hygromycin-resistant mammalian expression plasmids (Invitrogen, Carlsbad, CA, USA) to obtain plasmids expressing sense or antisense cDNAs. Antibodies for Akt, phospho-Akt, Erk, and phospho-Erk were obtained from Biosource International (Camarillo, CA, USA). All commercial antibodies were used in the dilutions indicated by the manufacturer.

Cell culture

The derivation of the M12 cell line has been previously described (Bae *et al.*, 1994, 1995, 1998; Jackson-Cook *et al.*, 1996). Briefly, human prostate epithelial cells were immortalized with SV40-T antigen to produce the poorly tumorigenic P69SV40 T (P69) cell line. P69 cells were injected subcutaneously into athymic nude mice, producing tumor nodules in 2/18 animals after 180 days. These nodules were reimplanted in athymic mice and after three passages resulted in the M12 cells, which demonstrated a short latency period of 7–10 days to tumor formation in 10/10 animals and were locally invasive and metastatic. Cells were cultured in RPMI-1640 medium supplemented with 10 ng/ml EGF, 0.02 mM dexamethasone, 5 µg/ml insulin, 5 µg/ml transferrin, 5 ng/ml selenium, fungizone, and gentamicin at 37°C under 5% CO₂. PC-3 and LNCaP cells were obtained from ATCC (Bethesda, MD, USA) and grown in the same medium as the M12 cells with the addition of 5% FBS. All cells used in these experiments were mycoplasma free, as determined by the Mycoplasma PCR Primer Set (Stratagene, La Jolla, CA, USA). Additional cell cultures were performed under reduced O₂ at 1 and 4% concentrations.

Transfection

The construction of the M12 cells with stable expression of mac25/IGFBP-rP1 has been previously described (Sprenger *et al.*, 1999). PC-3 and LNCaP mac25/IGFBP-rP1-expressing cells were constructed using the same mac25/IGFBP-rP1 pcDNA3 plasmid constructs used to make the M12 mac25/IGFBP-rP1 cell lines (Sprenger *et al.*, 1999). Transfection was done using Tfx20 (Promega, Madison, WI, USA). SOD-2 cDNA transfections were using Lipofectamine (GIBCO/Life Technologies, Rockville, MD, USA) performed as previously described (Sprenger *et al.*, 1999). Several clones from each transfection that were resistant to the selective antibiotic, G418, were selected and evaluated by Western and Northern blotting to assure appropriate gene expression or suppression. At least two clones from each transfection were used in subsequent experiments.

Western immunoblots

Media or cell lysates were collected as previously described (Sprenger *et al.*, 1999). After concentration of 1 ml medium onto nitrocellulose (Bio-Rad, Hercules, CA, USA) using a dot-blot apparatus, the proteins were redissolved in 50 µl SDS sample buffer (0.5 M Tris, pH 6.8, 1% SDS, 10% glycerol, 0.003% bromophenol blue, and 8 M urea) by heating for 10 min at 100°C as previously described (Birnbaum *et al.*, 1994). Samples were electrophoresed on 12% SDS-polyacrylamide gels (PAGE), then electroblotted onto nitrocellulose

(Bio-Rad, Hercules, CA, USA). Western blots were incubated in 0.3% Tween-20 in TBS overnight at 4°C. Mac25/IGFBP-rP1 antibody dilution was 1:3000, all other antibodies were diluted 1:1000. Bound antibody was detected using a horseradish peroxidase-linked donkey anti-rabbit secondary antibody and the ECL detection system according to the manufacturer's protocol. Buffers and wash times were as suggested by the manufacturer, except that the nitrocellulose was first washed with 10% H₂O₂ for 10 min. A measure of 40 µg of protein was loaded per lane unless otherwise specified.

RNA analysis

Cells were grown to approximately 80% confluence, at which time total RNA was isolated using an acid guanidinium thiocyanate/phenol/chloroform extraction method as previously described (Plymate *et al.*, 1996). Approximately 10 µg of each RNA preparation (quantitated by optical density at 260 nm) was separated by electrophoresis on a 1% agarose/6% (2.2 M) formaldehyde gel, transferred overnight by capillary action onto a nylon membrane (GeneScreen, DuPont, Wilmington, DE, USA), and crosslinked to the membrane by UV irradiation in a Stratalinker 1800 (Stratagene, LaJolla, CA, USA). Northern blot analysis was performed by hybridizing the membrane overnight with the mac25/IGFBP-rP1 or SOD-2 cDNA probe labeled with [³²P]dCTP to a specific activity of 10⁸ d.p.m./µg DNA by the random primers method. Hybridization was carried out at 42°C in a solution of 5 × Denhardt's solution with 50 µg/ml sonicated salmon sperm DNA and 50% deionized formamide. Following a final wash with 0.1 × SSC at 65°C, the blot was exposed to X-ray film (Kodak X-Omat-AR) with an intensifying screen at -80°C for 48–72 h.

Tumor formation in vivo

Groups of 10 nude, athymic male mice were injected subcutaneously with 10⁶ cells from the respective cell lines. All cell lines were injected in PBS except for the LNCaP cell line, which was injected with a 1:1 ratio of Matrigel™ and PBS. Mice were then monitored biweekly for tumor formation and weight gain/loss for 8 weeks. If tumors were present, tumor volume was calculated using the formula: $(l \times w^2)/2$ (where l = length and w = width of tumor). Statistical analyses using Kruskal–Wallis (for comparing the rate of tumor formation) and the Mann–Whitney U -test (for comparing tumor volumes) were then performed. After 8 weeks, the mice were killed and their tumors removed. These tumors were present, digested with 0.1% collagenase (Type I) and 50 µg/ml DNase (Worthington Biochemical Corp., Freehold, NJ, USA). Dispersed cells were plated in ITS medium/5% FBS at 5% CO₂, with 200 µg/ml G418, at 37°C for 24 h to allow attachment. When the cells had reached 80% confluence, they were split at a 1:4 ratio into 60 mm dishes. After the cells had reached 80% confluence, they were switched to serum-free medium and 24 h later media were collected and the cells in the dishes from which the media had been collected were counted. RNA was collected from separate plates using the RNeasy™ kit (Qiagen, Valencia, CA, USA). Media and RNA were collected and Western immunoblots and Northern blots were run to confirm that the tumor cells retained the mac25/IGFBP-rP1 phenotype of the injected cells.

Microarray fabrication

A nonredundant set of 6000 prostate-derived cDNA clones was identified from the Prostate Expression DataBase (PEDB), a

public sequence repository of expressed sequence tag (EST) data derived from human prostate cDNA libraries (Hawkins *et al.*, 1999). Preparation of PCR products onto glass slides has been previously described (Pritchard *et al.*, 2001).

Probe construction and microarray hybridization

Total RNA was isolated from each of the cell lines using TRIzol (Life Technologies). Fluorescence-labeled probes were made from 30 µg total RNA in a reaction volume of 20 µl containing 1 µl anchored oligo-dT primer (Amersham), 0.05 mM Cy3-dCTP (Amersham), 0.05 mM dCTP, 0.1 mM each dGTP, dATP, dTTP, and 200 U Superscript II reverse transcriptase (Life Technologies). Reactants were incubated at 42°C for 120 min followed by heating to 94°C for 3 min. Unlabeled RNA was hydrolyzed by the addition of 1 µl of 5N NaOH and heating to 37°C for 10 min. A volume of 1 µl of 5 M HCl and 5 µl of 1 M Tris-HCl (pH 7.5) were added to neutralize the base. Unincorporated nucleotides and salts were removed by chromatography (Qiagen), and the cDNA was eluted in 30 µl dH₂O. A measure of 1 µg of dA/dT 12–18 (Pharmacia) and 1 µg of human Cot1 DNA (Life Technologies) were added to the probe, heat denatured at 94°C for 5 min, combined with an equal volume of 2X microarray hybridization solution (Amersham) and prehybridized at 50°C for 1 h. The mixture was then placed onto a microarray slide with a coverslip and hybridized in a humid chamber at 52°C for 16 h. The slides were washed once with 1 × SSC, 0.2% SDS at room temperature for 5 min, then twice with 0.1 × SSC and 0.2% SDS at room temperature for 10 min.

Image acquisition and data analyses

Fluorescence intensities of the immobilized targets were measured using a laser confocal microscope (Molecular Dynamics). Intensity data were integrated at a pixel resolution of 10 µm using approximately 20 pixels per spot, and recorded at 16 bits. Quantitative data were obtained with the Spot-Finder V 2.4 program written at the University of Washington. Local background hybridization signals were subtracted prior to comparing spot intensities and determining expression ratios. For each experiment, each cDNA was represented twice on each slide, and the experiments were performed in duplicate producing four data points per cDNA clone per hybridization probe. Intensity ratios for each cDNA clone hybridized with probes derived from the respective cell line were calculated (mac25/IGFBP-rP1 intensity/control intensity). Gene-expression levels were considered significantly different between the two conditions if all four replicate spots for a given cDNA demonstrated a ratio >2 or <0.5, and the signal intensity was greater than 2 s.d. above the image background. We have previously determined that expression ratios less than 1.5 are not reproducible in our system (data not shown).

Promoter assay

The human SOD-2 promoter plasmid construct was a generous gift from Dr Moon Bin Yin (Bethesda, MD, USA) and consisted of a 3.6 kb pair from the SOD-2 gene containing the 5' flanking region to the transcription site, exon 1 and part of intron 1 (from -3340 to +260 nucleotide residues) ligated into the pGL3-basic vector (Kim *et al.*, 1999).

For the transient transfections, cells were plated in a 96-well plate at 1 × 10⁴ cells per well. At 80% confluence, the cells were transfected with the SOD-2 promoter/luciferase vectors using Tfx-20 according to the manufacturer's protocol (Promega). Briefly, each well received 0.1 µg vector DNA using a 3:1

charge ratio of Tfx-20/DNA to vector DNA in 40 μ l RPMI as determined by the manufacturer (Promega Co., Madison, WI, USA). After 1 h, 100 μ l of 1% serum-containing media was added and the cells were incubated for 24 h. Luciferase activity was then measured.

Luciferase activity was determined using the Luciferase Assay System (Promega). Cells were lysed with 20 μ l 1 \times reporter lysis buffer and luciferase activity was measured using a Wallac Inc. Victor² microplate reader (Perkin Elmer, Gaithersburg, MD, USA) with 100 μ l of luciferase assay buffer injected automatically and read for 10 s. Transfection efficiency was determined by transfection of triplicate wells with the pGL3 control vector in which luciferase expression is driven by the simian virus 40 promoter. The coefficient of variation of transfection was determined from five experiments of triplicate wells and was 1.9% CV with a transfection efficiency of 80 \pm 6% between experiments. Separate triplicate cells were transfected with a pGL3 basic luciferase reporter vector, lacking the SOD-2 insert and another promoter, which served as a nonspecific control.

SOD enzymatic activity

Total SOD activity was determined using 1 \times 10⁷–2 \times 10⁷ control or experimental cells that were rinsed with PBS, trypsinized and pelleted by centrifugation. Pellets were reconstituted in 100 μ l of water. Cells were then disrupted by three freeze–thaw cycles at –70°C. After the final thaw, pellets were spun at 3000 g at 4°C. A 1 : 10 dilution of the cell homogenate was then used for the assay. The SOD activity was measured using a kit from Calbiochem (San Diego, CA, USA). This assay measures the rate of oxidation of 5,6,6a,11b-tetrahydro-3,9,10-trihydroxybenzo(c)fluorene. The oxidation of this compound yields a chromophore that absorbs at 525 nm. The concentration of SOD activity is measured in SOD-525 units determined from the ratio of the velocity_{sample} : velocity_{control} compared to a ratio provided by the manufacturer.

Specific SOD-2 activity was determined by the method previously described by Sprenger *et al.* (2002).

Flow cytometry using propidium iodide

Flow cytometry was performed as previously described (Sprenger *et al.*, 2002). Briefly, cells were grown to 80% confluence. Cells (2 \times 10⁶) were pelleted and washed with PBS. Pellets were resuspended in cold 70% ethanol to a final density of 1 \times 10⁶ cells/ml, then pelleted and resuspended in 1 ml of DNA staining solution (PBS, pH 7.4, containing 0.1% Triton X-100, 0.1 mM EDTA (pH 7.4), 0.05 mg/ml RNase A (50 U/mg), and 50 μ g/ml propidium iodide). Cells were read on a Becton–Dickinson FACS Caliber at a wavelength of 488 nm. Data were collected and analysed using CellQuest and ModFit software, respectively.

GSH assay

Cell pellets were suspended in phosphate buffer (PB: 50 mM potassium phosphate buffer, pH 7.8), and a small aliquot was used for protein quantitation. For glutathione assay, protein

precipitation was carried out by mixing one volume of cell suspension with one volume of 10% 5-sulfosalicylic acid and centrifuged at 15 000 r.p.m. for 5 min at 4°C. The supernatants were collected and total glutathione was measured in a DU640 spectrophotometer (Beckman) as previously described (Li *et al.*, 1998a). Oxidized glutathione was indirectly estimated by measuring reduced glutathione after the supernatants were incubated in 2-vinylpyridine for 90 min at 4°C.

Cell growth assay

The growth rate of each cell type and clone was determined by counting the number of cells as a function of time. Cells were incubated at 37°C, 5% CO₂. Before counting, medium was aspirated, 3 ml of 1 \times PBS was added and aspirated, and 2 ml of 1 \times trypsin was added to each well. Cells were incubated for 10 min at 37°C, 5% CO₂. A volume of 3 ml appropriate medium was added to each well and cells were triturated. Cells were then spun for 3 min at 10 000 r.p.m. followed by reconstitution in a 10 ml medium. Cells were seeded into six-well plates at 2.5 \times 10⁵ cells/well containing 2 ml of appropriate culture medium. Three parallel wells for each of the control and experimental cells, clones A and B, were seeded for each time point. Cells were counted at 24, 48, 72, and 96 h using a hemocytometer. Cells at 1 and 4% O₂ were counted in a similar manner.

Apoptosis

Caspase 3/7 (DEVDase) activity for each cell type and clone was measured using the Apo-ONE homogenous Caspase-3/7 Assay (Promega, Madison, WI, USA) according to the manufacturer's directions, at two time points. Cells were seeded in black-bottomed 96-well plates at 2.5 \times 10³ cells/well containing 100 μ l of culture medium (RPMI, transferrin and selenium). A total of 16 parallel wells for each cell type and clone were seeded for each time point. Cells were incubated at 37°C, 5% CO₂. At 48 and 96 h, 100 μ l of Caspase 3/7 Reagent was added to each well of separate plates. These plates were covered with foil, placed on shaker, and read 2.5 h later on a Wallac Victor² 1420 fluorescent plate reader at an excitation wavelength of 485 nm and an emission wavelength of 530 nm. Apoptosis was also assessed by PARP cleavage. In this assay cells were grown in 60 mm dishes. At 24 h after plating in complete medium, cells were changed to RPMI-1640 + transferrin and selenium. Both floating and adhered cells were collected from separate plates at 48 and 96 h after complete medium was removed. Cell lysates were collected and run on a 7.5% SDS PAGE. Western immunoblots were performed with an anti-polyadenosylribose polymerase (PARP) antibody that recognizes the 85 kDa cleaved fragment (Promega Co., Madison, WI, USA).

Acknowledgements

The study was supported by the Veterans Affairs Research Service and DOD to SRP and TDO, and NIH DK52683 and PO1-CA 85859 to SRP.

References

- Bae V, Jackson-Cook C, Brothman A, Maygarden S and Ware J. (1994). *Int. J. Cancer*, **58**, 721–729.
- Bae V, Jackson-Cook C, Maygarden S, Chen J, Plymate S and Ware J. (1998). *Prostate*, **34**, 275–282.

- Bae V, Jackson-Cook C, Maygarden S, Edelman W, Brothman A, Chen J and Ware J. (1995). *Proc. Amer. Assoc. Cancer Res., Cancer Res.*, **642** (abstract), 55.
- Baker A, Oberley L and Cohen M. (1997). *Prostate*, **32**, 229–233.

- Birkenkamp KV, Dokter WHA, Esselink MT, Jonk LUC, Kruijer W and Vellenga E. (1999). *Leukemia*, **13**, 1037–1045.
- Birnbaum R, Ware J and Plymate S. (1994). *J. Endocrinol.*, **141**, 535–540.
- Bost F, Caron L, Marchetti I, Dani C and Le Marchand-Brustel Y. (2002). *J. Biochem.*, **361**, 621–627.
- Bostwick D, Alexander E, Singh R, Shan R, Qian J, Santella R, Oberley L, Yan T, Zhong W, Jiang X and Oberley T. (2000). *Am. Cancer Soc.*, **89**, 123–134.
- Chen Q, Bartholomew J, Campisi J, Acosta M, Reagan J and Ames B. (1998). *J. Biochem.*, **332**, 43–50.
- de Haan J, Cristiano F, Iannello R, Bladier C, Kelner M and Kola I. (1996). *Hum. Mol. Genet.*, **5**, 283–292.
- Hawkins V, Doll D, Bumgarner R, Smith T, Abajian C, Hood L and Nelson P. (1999). *Nucleic Acids Res.*, **27**(1), 204–208.
- Huang C, Zhang Z, Ding Z, Li J, Ye J, Leonard S, Shen H-M, Butterworth L, Lu Y, Costa M, Rojanasakul Y, Castranova V, Vallyathan V and Shi X. (2000). *J. Biol. Chem.*, **275**, 32516–32522.
- Hwa V, Oh Y and Rosenfeld R. (1998a). *Acta. Ped. Scand.*, **428**, 37–45.
- Hwa V, Tomasini-Sprenger C, Bermejo A, Rosenfeld R and Plymate S. (1998b). *J. Clin. Endocrinol.*, **83**, 4355–4362.
- Jackson-Cook C, Bae V, Edelman W, Brothman A and Ware J. (1996). *Cancer Genet. Cytogen.*, **87**, 14–23.
- Kim K, Rodriguez A, Carrico P and Melendez J. (2001). *Antioxidants Redox Signal.*, **3**, 361–373.
- Kim H-P, Roe J-H, Chock P and Yim M. (1999). *J. Biol. Chem.*, **274**, 37455–37460.
- Kinscherf R, Claus R, Wagner M, Gehrke C, Kamencic H, Hou D, Nauen O, Schmiedt W, Kovacs G, Pill J, Metz J and Deigner H. (1998). *FASEB J.*, **12**, 461–467.
- Li N, Oberley T, Oberley L and Zhong W. (1998a). *J. Cellular Physiol.*, **175**, 359–369.
- Li N, Oberley T, Oberley L and Zhong W. (1998b). *Prostate*, **35**, 221–223.
- Lopez-Bermejo A, Buckway C, Devi G, Hwa V, Plymate S, Oh Y and Rosenfeld R. (2000). *Endocrinology*, **141**, 4072–4080.
- McCord J. (2000). *Am. J. Med.*, **108**, 652–659.
- Oberley L. (2001). *Antioxidants Redox Signal.*, **3**, 461–472.
- Oberley TD and Oberley LW. (1997). *Histol. Histopathol.*, **12**, 525–535.
- Oh Y, Nagalla R, Yamanaka Y, Kim H, Wilson E and Rosenfeld R. (1996). *J. Biol. Chem.*, **271**, 30322–30325.
- Plymate S, Ware J, Tennant M, Thrasher J, Chatta K and Birnbaum R. (1996). *J. Clin. Endocrinol. Metab.*, **81**, 3709–3716.
- Pritchard C, Hsu L, Delrow J and Nelson P. (2001). *Proc. Natl. Acad. Sci. USA*, **98**, 13266–13271.
- Rhee S, Bae Y, Lee S-R and Kwon J. (2000). *Science's Signal Transduction Knowledge Environment*, www.stke.org/cgi/content/full/OC_sigtrans;2000/53/pe1, pp. 1–4.
- Sachdeva R, Martin A-M, Heyworth M, Zeigler-Johnson C, Spangler E, Wilker A, Malkowicz S and Rebbeck T. (2001). *Am. J. Hum. Genet.*, **69**(4), 261.
- Sprenger C, Damon S, Hwa V, Rosenfeld R and Plymate S. (1999). *Cancer Res.*, **59**, 2370–2375.
- Sprenger C, Vail M, Evans K, Simurdak J and Plymate S. (2002). *Oncogene*, **21**, 140–147.
- Wartenberg M, Diedershagen H, Hescheler J and Sauer H. (1999). *J. Biol. Chem.*, **39**, 27759–27767.
- Widmann C, Gerwins P, Johnson N, Jarpe M and Johnson G. (1998). *Mol. Cell. Biol.*, **18**, 2416–2429.
- Wilson E, Oh Y, Hwa V and Rosenfeld R. (2001). *J. Clin. Endocrinol. Metab.*, **86**, 4504–4511.
- Zhong W and Oberley T. (2001). *Cancer Res.*, **61**, 7071–7078.